# MATHEMATICAL MODELLING OF ETHANOL DEHYDRATION FROM AZEOTROPIC CONCENTRATION USING PRESSURE SWING ADSORPTION (PSA) PROCESS

**E. T. Evwierhoma[1], A. Jaiyeola[1], A. B. Ehinmowo[1] and P. I. Babalola[1]**

[1]Department of Chemical and Petroleum Engineering,
University of Lagos, Lagos-Nigeria.

Article History: Received 4.6.2017; Revised 18.9.2018; Accepted 11.12.2018

***ABSTRACT***

*The demand for pure ethanol has become paramount for its various applications in biofuels and preparation of industrial chemicals, food and pharmaceutical products. Pressure Swing Adsorption (PSA) has proven to be an effective process and a more economical method for separating the azeotropic concentration of ethanol-water (95% ethanol, 5% water) than distillation. The modeling of PSA of ethanol-water azeotropic concentration on zeolite 3A was done. The unsteady state mass balance equation for the water molecule in the packed bed was done as well. The sets of Partial Differential Equations obtained from the model equations were solved with the Crank Nicholson finite difference method using MATLAB software. The simulated data was observed to be considerably in agreement with the experimental data. The data obtained for dimensionless bed length z = 0.1 explains better the experimental result with Least Sum of Square Residuals (LSSR) of 0.06588. Breakthrough time of 600 seconds was obtained from simulated data while that of experimental was 680 seconds. The purity of 99.2705% v/v anhydrous ethanol was obtained.*

***KEYWORDS**: Biofuel; anhydrous ethanol; adsorption; breakthrough time*

## 1.0 INTRODUCTION

Ethanol, over the years has been an important feedstock in the chemical industry for the preparation and synthesis of other important chemicals due to its high miscibility with water and other chemicals. Its use as a fuel and gasoline additive has increased its demand. With this rise in demand also arose the need for the need to obtain its anhydrous form which requires the removal of water from its azeotropic concentration. Ethanol boils at 78.4°C, water boils at 100°C. Ethanol forms a constant-boiling mixture, or azeotrope, with water

* Corresponding author: eevwierhoma@unilag.edu.ng

that contains 95% ethanol and 5% water and that boils at 78.15°C; since the boiling point of this binary azeotrope is below that of pure ethanol, absolute ethanol cannot be obtained by simple distillation.

Whatever method of preparation of ethanol used – synthesis from ethane using steam, fermentation of sugars and starches using yeast or fermentation from biomass using bacteria, the ethanol obtained is usually in a mixture with water.

The ethanol is then extracted from this solution by fractional distillation, according to Seader, Henley and Roper (2011). Distillation is usually the method of choice; however, water cannot be completely removed due to the presence of the azeotrope. Ethanol forms a positive azeotrope which boils at a lower temperature than either of its constituents. but the azeotrope boils at 78.2°C, which is lower than either of its constituents. Positive azeotropes are also called minimum boiling mixtures.

Several methods have been developed to break the ethanol-water azeotropic concentration. Though these techniques have been effective in obtaining high purity ethanol, they had their various disadvantages of high energy consumption and involving the use of entrainers that are not environmentally friendly (Seader, et. al. 2011).

At high pressure, gas molecules are preferentially adsorbed onto the adsorbent material depending on their molecular characteristics and affinity for the adsorbent; when the pressure is lowered, the adsorbed molecules are released (desorbed). Pressure swing adsorption (PSA) allows desorption to occur at a pressure much lower than normal adsorption. Reduction of pressure is used to shift the adsorption equilibrium and affect regeneration of the adsorbent. The cost effectiveness of pressure swing adsorption is due to its cycles operating at constant temperature, requiring no heating or cooling steps and the use of exothermic heat of adsorption remaining in the adsorbent to supply the endothermic heat needed for desorption. PSA cycles are characterized by high residual loadings and because particles of adsorbent respond quickly to changes in pressure, then cycles turns are necessarily short for reasonably sized-beds (seconds to minutes). Jeong, Jeon, Chung and Choi (2012) found out that dehydration of ethanol at azeotropic conditions (93 - 96 % v/v) using the Pressure Swing Adsorption (PSA) with Molecular Sieve columns offers significant economic and environmental advantages, compared to traditional ternary distillation processes. Traditional distillation to obtain anhydrous ethanol is a highly energetic process. Adsorption as a low energy consumption process

attracts more attention for the final separation of ethanol-water azeotrope since it requires relative low energy input and is capable of producing a product of very high purity.

Pressure swing adsorption has been proven to be a promising technique in breaking azeotropes with the advantage that column pressure can be changed faster than the column temperature. The fast changes in pressure enable short cycle times and thus much higher throughput per unit of adsorbent bed volume is possible in the case of PSA compared to the thermal swing adsorption, TSA, system. As a result, the productivity of a PSA system defined as the amount of dry ethanol produced per hour per ton of adsorbent is much higher (Saenghdhan & Apichat (2011); Elzbieta, Nastaj, Tabero & Aleksandrzak, 2015). Chopade, Khadetoid and Mohod (2015) claimed that pressure swing adsorption is an energy efficient form of separation in ethanol-water azeotropic concentration using zeolite 3A as compared with other methods of separation. The zeolite 3A molecular sieve has a nominal pore size of 3 Angstroms and it allows the penetration of water molecules whose diameter is 2.8 Angstroms. The ethanol molecule whose average diameter is 4.4Angstroms is rejected by the sieve (Chopade et al., 2015).

In ethanol water azeotropic mixture, the boiling point and composition curve have a lower value than the boiling points of either water or ethanol. This minimum occurs with 95.6% by mass of ethanol in the mixture at a boiling point of 78.20C, compared with the boiling point at 78.5oC and water at 100oC. At this point, it is impossible to obtain pure ethanol and water containing more than 95.6% of ethanol with further distillation because the liquid composition is the same with the vapor composition. This is known as a constant boiling mixture or azeotrope. However, the azeotropic composition as well as its boiling point changes with pressure. The PSA process is attractive due to its low energy consumption and no solvent nor entrainer is needed (Jeong et al., 2012). It has been shown by Okewale (2013) that ethanol dehydration by adsorption requires far less energy than the conventional azeotropic distillation.

This work focused on the study of pressure swing adsorption concept and its application to the removal of water from azeotropic concentration (95%ethanol, 5%water, adsorbed on zeolite 3A molecular sieve) of ethanol. This was achieved through the development of mathematical model and simulation of the pressure swing adsorption of water.

### 1.1 Pressure Swing Adsorption

PSA processes involve adsorption of components of a mixture by solid adsorbent at a relatively high pressure. These usually occur through gas-solid contact in a packed column so as to produce a stream enriched in less strongly adsorbed components of the feed gas. Then the adsorbed components are desorbed by reducing the partial pressures of the adsorbed phase in another column. The desorbed components are obtained without additional energy cost.

A PSA process cycle is complete when adsorption is followed by desorption. Reduction of pressure is used to shift the adsorption equilibrium and affect regeneration of the adsorbent. In a PSA process cycle, regeneration is achieved by a depressurization that must reduce the partial pressure of the adsorbates to allow desorption. The cycles operate at constant temperature, requiring no heating or cooling steps. Rather, they use the exothermic heat of adsorption remaining in the adsorbent to supply the endothermic heat required for desorption. PSA is most often equilibrium controlled almost isothermal process with pressure swing between two extreme pressures. Usually the production step is taking place at the highest pressure and the bed is generated by decreasing the partial pressure of the adsorbed component(s).

PSA processes operate at ambient temperatures and do not require solvent for product recovery or adsorbent regeneration. As a result, their capital expenditure is quite less compared to cryogenic and fractional distillation techniques.

A lot of micro-porous materials are available and more are being synthesized and optimized lattice composition and pore architecture contribute to beneficial adsorption (Jochem &Helmut, 2012).

Ethanol is produced usually by fermentation of starch obtained from seeds and stems such as corn, sugar beets and sugarcane. However, the dominant feedstock is sugarcane. The fermentation based process is more attractive due to the impending shortage of petroleum feed stocks and the fact that the raw material for fermentation is renewable.

The need for further purification of the azeotropic concentration is to produce a high grade ethanol that can be blended with gasoline.

The energy required for the product purification is the most significant cost involved in the ethanol production process. The ethanol obtained by fermentation can be enriched up to maximum of 95wt% (azeotrope concentration). Further enrichment of ethanol must break this azeotropic concentration by other means (Delgado, Agueda, Ugama, Sotelo, Garcia-Sanz & Darcia, 2015). PSA has been very helpful in this regard.

In recent years, the demand for ethanol had risen up highly as petroleum-based fuel became expensive and environmental concerns involving leaded gasoline created a need for a replacement and fuel with higher octane.

## 2.0 METHODOLOGY

### 2.1 Mathematical Models of PSA

This work used the azeotrope mixture of ethanol-water system (95%ethanol, 5%water), adsorbed on zeolite 3A molecular sieve. The separation of water from the azeotropic concentration of ethanol water by pressure swing adsorption is mainly based on the preferential adsorption of water on a porous adsorbent. Therefore, zeolite 3A, a suitable industrial adsorbent for separation, was used as adsorbent due to its high adsorption capacity for water (Chopade et al., 2015,).

One can generally summarize the highlights of the models of various types according to the following aspects claimed by Grande and Blom (2012): -

- The fluid flow pattern (generally plug flow or axially dispersed plug flow).
- Constant or variable fluid velocity.
- The form of the equilibrium relationship(s).
- The form of the kinetic rate expression(s).
- The inclusion of heat effects(isothermal/nonisothermal)
- The numerical methods used to solve

### 2.2 Development of the Adsorption Model.

In order to derive the mass balance equation for the steady state concentration distribution of the water molecule in the ethanol-water concentration along a packed bed, we consider a thin slice of the unit cross section of the bed with thickness of $\Delta z$ at a distance $z$ from the feed end of the bed (The volume of the slice is taken to be $\Delta z$)

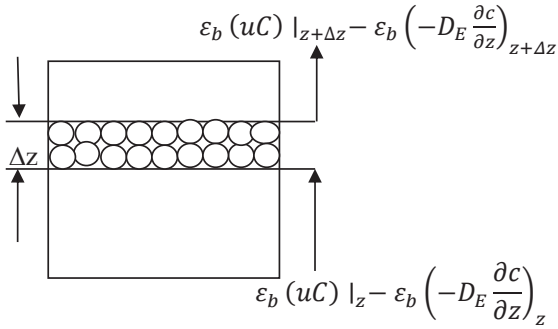


Figure 1. A section of a packed bed adsorption column

The solute(water molecule) entering the slice at any time t will

- Be partly adsorbed in the slice
- Partly accumulated at the interstitial fluid in the slice and
- Partly outflow from the slice by bulk flow and axial dispersion.

Using the law of conservation of mass, the following expressions as given in Equations (1a) to (3) apply: -

Rate of input of the water molecule to the slice (atz) = $\varepsilon_b\,(uC)\,|_z$

Rate of output of the water molecule from the slice at (z+Δz) = $\varepsilon_b\,(uC)\,|_{z+\Delta z}$

Rate of removal of the solute from the gas by adsorption in the slice by axial dispersion

$$=\varepsilon_b\left(-D_E\frac{\partial c}{\partial z}\right)_z \tag{1a}$$

Rate of removal of the solute from the gas y adsorption in the slice = $\Delta z(1-\varepsilon_b)\bar{a}J_o$

Rate of accumulation of the solute in the interstitial fluid = $\varepsilon_b\ \Delta z\left(\frac{\partial c}{\partial t}\right)$

An unsteady state mass balance over the slice yields

$$\varepsilon_b\,(uC)\,|_z - \varepsilon_b\left(-D_E\frac{\partial c}{\partial z}\right)_z - (\varepsilon_b\,(uC)\,|_{z+\Delta z} - \varepsilon_b\left(-D_E\frac{\partial c}{\partial z}\right)|_{z+\Delta z})$$
$$= \Delta z(1-\varepsilon_b)\bar{a}J_o \ + \varepsilon_b\ \Delta z\left(\frac{\partial c}{\partial t}\right) \tag{1b}$$

Dividing by Δz throughout and taking the limit $\Delta z \to 0$

$$\varepsilon_b D_E\frac{\partial^2 c}{\partial z^2} - \varepsilon_b u\frac{\partial c}{\partial z} - (1-\varepsilon_b)\bar{a}J_o = \varepsilon_b\frac{\partial c}{\partial t} \tag{2}$$

$$D_E \frac{\partial^2 c}{\partial z^2} - u\frac{\partial c}{\partial z} - \frac{3(1-\varepsilon_b)}{\varepsilon_b r_o} k_c\big(C - C(r_o)\big) = \frac{\partial c}{\partial t} \tag{3}$$

Here, $k_c$ = the mass transfer coefficient at the external surface of a pellet.

$J_o$ = solute flux i.e $J_o$ = ($C$-$C(r_o)$) where $C(r_o)$ is the solute concentration at the pore mouth $r = r_o$ (the solute concentration at the pellet surface).If $\bar{q}$ is the average concentration of the solute in a pellet, Equation (3) can be written in an alternative form,as given in Equation (4) below:-

$$D_E \frac{\partial^2 c}{\partial z^2} - u\frac{\partial c}{\partial z} - \frac{(1-\varepsilon_b)}{\varepsilon_b}\rho_p \frac{\partial \bar{q}}{\partial t} = \frac{\partial c}{\partial t} \tag{4}$$

In this present study, the proposed theoretical model considers a separation system of water from ethanol-water azeotrope through the PSA process in a fixed bed (packed column) (Jeong et al 2014; Baylak, Kumar, Ni & Dalai, 2012).

The following assumptions were made:

- The process is a binary system of ethanol and water
- Axially dispersed plug flow (The axial diffusion effect is accounted for, that is, not negligible)
- Extended Langmuir isotherm is employed as the equilibrium adsorption model
- The process is considered isothermal (constant temperature)
- Negligible pressure drop
- Negligible radial gradients
- Ideal gas behavior
- Uniform adsorbent properties along the axial coordinate and uniform cross sectional void fraction

Based on these assumptions, the mass balance for component $i$ is given by Equation (5) as below:-

$$\frac{\partial C_i}{\partial t} = D_E \frac{\partial C_i}{\partial Z^2} - U\frac{\partial C_i}{\partial z} - \left(\frac{1-\varepsilon_b}{\varepsilon_b}\right)\rho_p \frac{\partial q_i}{\partial t} \; i = 1, \ldots\ldots\ldots\ldots n \tag{5}$$

The first, second and third term represent the accumulation, the convective mass transfer, and the diffusion in the gas phase respectively. The last term describes the mass transfer between the adsorbent and fluid phase due to adsorption or desorption

With the initial condition as given in Equation (6), whereby

At t = 0; c = 0 (6)

and boundary conditions as given in Equations (7) and (8) as follow: -

$$At\ z = 0\ ;\ C_{in} = C - \frac{D_E}{U}\frac{\partial C}{\partial z} \tag{7}$$

$$At\ z = L\ ;\ \frac{\partial C}{\partial z} = 0 \tag{8}$$

The last term of equation (5) is determined as in Equation (9) as follow: -

$$\frac{\partial q_i}{\partial t} = k_i\ (q_i^*\ - q_i) \tag{9}$$

Where $k_i$ is the mass transfer coefficient.

The Langmuir isotherm is used to describe the equilibrium relationship

$$q_i^* = \frac{q_m\, b_i P_i}{1 + \sum_{i=1}^{n} b_i\, P_i} \tag{10}$$

$q_m$ = *total site* (Langmuir parameter)

Also, the Langmuir parameter can be expressed as in Equations (11) and (12) below: -

$$q_{mi} = t_1 + t_2 T \tag{11}$$

$$b_i = t_3\ \exp(\ t_4/T) \tag{12}$$

To solve the resulting partial differential equations, they are first converted into dimensionless forms as given in Equations (13 to (1) as follows: -

Taking the dimensional variables to be

$$\bar{t}\ = \frac{ut}{L}\ , \qquad \bar{z} = \frac{z}{L}\ , \qquad \bar{C_\iota} = \frac{C_i}{C_{io,in}}$$

Therefore,

$$\frac{\partial C_i}{\partial t}\ =\ D_E\frac{\partial C_i}{\partial Z^2} -\ U\frac{\partial C_i}{\partial z} -\ \left(\frac{1-\varepsilon_b}{\varepsilon_b}\right)\rho_p\ \frac{\partial q_i}{\partial t} \qquad i = 1, \ldots\ldots\ldots\ldots n \tag{13}$$

Initial and boundary conditions:

t = 0 ; c = 0 (14)

$$At\ z = 0\ ;\ C_{in} = C - \frac{D_E}{U}\frac{\partial C}{\partial z} \tag{15}$$

$$At\ z = L\ ;\ \frac{\partial C}{\partial z} = 0 \tag{16}$$

Using dimensionless variables: $t = \frac{L\bar{t}}{U}$ , $z = \bar{z}L$ ; $\overline{C}_\iota = \frac{C_i}{C_{io,in}}$ (17)
$C_{io,in} = C_{io}$

Converting Equation (13) to dimensionless terms, we obtain

$$\frac{\partial C_i}{\partial t} = D_E\ \frac{\partial^2 C_i}{\partial z^2} - u\frac{\partial C_i}{\partial z} - \left(\frac{1-\varepsilon_b}{\varepsilon_b}\right)\rho_p\ K_i\ (q^*\ - q_i) \tag{18}$$

Where

$$\frac{\partial q_i}{\partial t} = k_i\ (q_i^*\ - q_i) \tag{19}$$

In which

$$\bar{q}_i\ = \frac{q_i}{C_{io}}\rho_p\ and\ \bar{q}^*{}_i\ = \frac{q_i^*}{C_{io}}\rho_p$$

Since

$$q_i^*\ = \frac{C_{io}q_i^*}{\rho_p} \text{If} \qquad K_i\ = \frac{u\overline{K}_i}{L},$$

Therefore, it can be shown that the expression in Equations (20) and (21) apply, as follow: -

$$\overline{K}_\iota = L\frac{K_i}{U} \tag{20}$$

$$\frac{UC_{io}}{L}\left(\frac{\partial \bar{C}_i}{\partial t}\right) = \frac{D_E\,C_{io}}{L^2}\frac{\partial^2 C_i}{\partial c^2}\ - \frac{UC_{io}}{L}\frac{\partial \bar{C}_i}{\partial \bar{z}} - \left(\frac{1-\varepsilon_b}{\varepsilon_b}\right)\rho_p\ \frac{C_{io}}{\rho_p}(\bar{q}_i^* - \bar{q}_i) \tag{21}$$

Multiplying through by $\frac{L}{C_{io}}$ and dividing by U, where $D_E\ \propto \frac{1}{Pe}$, equation (21) becomes an expression as given in Equation (22) as below:-

$$\left(\frac{\partial \bar{C}_i}{\partial t}\right) = \left(\frac{1}{Pe}\right)\frac{\partial^2 C_i}{\partial c^2}\ - \frac{\partial \bar{C}_i}{\partial \bar{z}} - \left(\frac{1-\varepsilon_b}{\varepsilon_b}\right)K_i\ (q^*\ - q_i) \tag{22}$$

Also, assuming that the expression in Equation (9) is dimensionless, it can be rewritten as in Equation (23) below: -

$$\frac{uC_{io}}{\rho_p\,L}\frac{\partial \bar{q}_i}{\partial t} = \bar{k}_i\ \frac{u}{L}(\bar{q}_i^*\ - \bar{q}_i)\frac{C_{io}}{\rho_p} \tag{23}$$

Therefore, the following expression in Equations (24) is considered, as below: -

$$\frac{\partial \bar{q}_i}{\partial t} = \bar{k}_i\ (\bar{q}_i^*\ - \bar{q}_i) \tag{24}$$

Equations (22) and (24) are solved alongside boundary and initial conditions and equilibrium data.

$$\text{At } t = 0 \;; c = 0 \;;\; \bar{t} = 0; \bar{C}_i = 0$$
$$z = 0;\; C_{in} = C - \frac{D_{Ei}}{u}\frac{\partial C}{\partial z} \tag{25}$$

From Equation. (3); writing for $i$ components and making dimensionless, the expressions in Equations (26) and (27) are considered, as follows: -

$$z = 0; C_{i,in(0)} = C_i - \frac{D_{Ei}}{u}\frac{\partial C_i}{\partial z} \;; = \; \bar{C}_{i,in} C_{i,o}$$

Therefore,

$$\bar{z} = 0; C_{io}\bar{C}_{i,in(0)} = C_{io}\bar{C}_i - C_{io}\frac{D_{Ei}}{Lu}\frac{\partial \bar{C}_i}{\partial \bar{z}}$$

$$\bar{z} = 0; \bar{C}_{i,in(0)} = \bar{C}_i - \frac{D_{Ei}}{Lu}\frac{\partial \bar{C}_i}{\partial \bar{z}} \text{ where Pe=peclect number}$$

$$Pe = \frac{uL}{D_E} \tag{26}$$

$$\bar{z} = 0; \bar{C}_{i,in(0)} = \bar{C}_i - \frac{1}{Pe}\frac{\partial \bar{C}_i}{\partial \bar{z}} \tag{27}$$

Also, Equation (8) can be rewritten as an expression in Equation (28) as follow: -

$$\bar{z} = L;\; \frac{\partial C_i}{\partial z} = 0;\; \bar{z}L = L;\; z = 1;\; \frac{\partial \bar{C}_i}{\partial \bar{z}} = 0 \tag{28}$$

### 2.3 Equilibrium relationship

Langmuir isotherm is considered, with the expression given in Equation (29) below: -

$$q_i^* = \frac{q_m\, b_i P_i}{1 + \sum_{i=1}^{n} b_i\, P_i} \tag{29}$$

whereby $q_m$ = total site (*langmuir parameter*)

Making Equation (29) dimensionless, the equation can be rewritten as in the expression in Equation (30) as follows: -

$$\frac{C_{io,in}\,\bar{q}_i^*}{\rho_p} = \frac{q_{mi} b_i\,(RT) C_{io,in}\bar{C}_i}{1 + RT\sum_{j=1}^{n} b_j C_{jo,in}\bar{C}_j} \tag{30}$$

Where P = cRT, therefore, the following expression in Equation (31) applies, as below: -

$$\bar{q}_i^* = \frac{q_{mi} b_i (RT) \bar{C}_i}{1 + RT \sum_{j=1}^{n} b_j C_{jo,in} \bar{C}_j} \tag{31}$$

Also, the Langmuir parameter can be represented as given in Equations (32) to (33) below: -

$$q_{mi} = t_1 + t_2 T \tag{32}$$

$$b_i = t_3 \exp(t_4/T) \tag{33}$$

in which the following parameters apply:-

$t_1 = \frac{mmol}{g}$
$t_2 = \frac{mmol}{gk}$
$t_3 = atm^{-1}$
$t_4 = K$

## 3.0 APPLICATION OF MODEL TO BINARY SYSTEM (Ethanol and Water System)

Writing for a binary system of water and ethanol, equation (22) becomes the following expressions in Equations (34) to (36): -

$$\frac{\partial \bar{C}_1}{\partial t} = \left(\frac{1}{Pe_1}\right)\frac{\partial^2 \bar{C}_1}{\partial c^2} - \frac{\partial \bar{C}_1}{\partial \bar{z}} - \beta_1\left(\bar{q}_1^* - \bar{q}_1\right) \tag{34}$$

$$\frac{\partial \bar{C}_2}{\partial t} = \left(\frac{1}{Pe_2}\right)\frac{\partial^2 \bar{C}_2}{\partial c^2} - \frac{\partial \bar{C}_2}{\partial \bar{z}} - \beta_2\left(\bar{q}_2^* - \bar{q}_2\right) \tag{35}$$

where $\beta_i = \left(\frac{1-\varepsilon_b}{\varepsilon_b}\right)\overline{K}_i$ (36)

Also, equation (24) becomes an expression as given in Equations (37) to (38) below:-

$$\frac{\partial \bar{q}_1}{\partial \bar{t}} = \bar{k}_1\ (\bar{q}_1^* - \bar{q}_1) \tag{37}$$

$$\frac{\partial \bar{q}_2}{\partial \bar{t}} = \bar{k}_2\ (\bar{q}_2^* - \bar{q}_2) \tag{38}$$

Subject to initial and boundary conditions, the following expressions are considered, as given in Equations (39) to (42) as follows:-

$$\bar{t} = 0; \bar{C}_1 = 0; \bar{C}_2 = 0 \tag{39}$$

where $C_{i,in} = C_{i,0}$

$$\bar{z} = 0; \bar{C}_{1,in} = \bar{C}_1 - \frac{1}{Pe_1}\frac{\partial \bar{C}_1}{\partial \bar{z}} \quad (40)$$

$$\bar{z} = 0; \bar{C}_{2,in} = \bar{C}_2 - \frac{1}{Pe_2}\frac{\partial \bar{C}_2}{\partial \bar{z}} \quad (41)$$

$$z = 1; \ \frac{\partial \bar{C}_1}{\partial \bar{z}} = 0 \ \ ; \ \frac{\partial \bar{C}_2}{\partial \bar{z}} = 0 \quad (42)$$

And for the equilibrium relationship;

$$\bar{q}_1^* = \frac{q_{m1} b_1 (RT) \bar{C}_1}{1 + RT\left(b_1 C_{10,in} \bar{C}_1 + b_2 C_{20,in} \bar{C}_2\right)} \quad (43)$$

$$\bar{q}_2^* = \frac{q_{m2} b_2 (RT) \bar{C}_2}{1 + RT\left(b_1 C_{10,in} \bar{C}_1 + b_2 C_{20,in} \bar{C}_2\right)} \quad (44)$$

$$q_{m1} = t_{1_1} + t_{1_2} T \ \ and \ \ q_{m2} = t_{2_1} + t_{2_2} T \quad (45)$$

$$b_1 = t_{1\,3} \exp(t_{1_4}/T) \ \ and \ \ b_2 = t_{2\,3} \exp(t_{2_4}/T) \quad (46)$$

Due to strong polar attraction between water molecules and hydroxyl groups of the adsorbent, water can adsorb faster and stronger than ethanol, therefore this system is considered as a single component. The single component adsorption is therefore described with the following expressions given in Equations (47) to (54) as follow: -

$$\frac{\partial \bar{C}_1}{\partial t} = \left(\frac{1}{Pe_1}\right)\frac{\partial^2 \bar{C}_1}{\partial c^2} - \frac{\partial \bar{C}_1}{\partial \bar{z}} - \beta_1\left(\bar{q}_1^* - \bar{q}_1\right) \quad (47)$$

$$\frac{\partial \bar{q}_1}{\partial \bar{t}} = \bar{k}_1 \ (\bar{q}_1^* - \bar{q}_1) \quad (48)$$

The boundary conditions are as given in Equations (49) to (54) below: -

$$\bar{t} = 0; \bar{C}_1 = 0; \quad (49)$$

$$\bar{z} = 0; \bar{C}_{1,in} = \bar{C}_1 - \frac{1}{Pe_1}\frac{\partial \bar{C}_1}{\partial \bar{z}} \quad (50)$$

$$z = 1; \qquad \frac{\partial \bar{C}_1}{\partial \bar{z}} = 0 \quad (51)$$

$$\bar{q}_1^* = \frac{q_{m1} b_1 (RT) \bar{C}_1}{1 + RT\left(b_1 C_{10,in} \bar{C}_1\right)} \quad (52)$$

$$q_{m1} = t_{1_1} + t_{1_2} T \quad (53)$$

$$b_1 = t_{1\,3} \exp(t_{1_4}/T) \quad (54)$$

## 4.0 METHOD OF NUMERICAL SOLUTION

Many methods of numerical analysis have been earlier discussed. For this present work, the Crank-Nicholson Finite difference method was used.

### 4.1 The Crank-Nicholson Finite Difference Method

The Crank-Nicholson method is based on a convex combination of the spatial terms of the forward and backward difference method. Although the method involves some computation, it has a high level of accuracy for linear and parabolic partial differential equation and it is unconditionally stable. It is also convenient in locating grid points or element where the solution has large gradients. This method also allows a larger time step than can be used in the explicit method (Sandip, 2015).

#### *4.1.1 Explicit Method*

In order to solve the problem, $x$ and t are discretized and the equations were solved

The basis for the Crank-Nicholson algorithm is, writing the final difference equation at a mid-level in time: $i, j + \frac{1}{2}$. The finite difference $x$ derivative at $j + \frac{1}{2}$ is computed as the average of the two central difference time derivatives at j and $j$+1.

Consider the boundary-initial value problem for transient heat conduction in a rod, with the ends held at zero temperature and an initial temperature profile $f(x)$, the following expressions apply, as given in Equations (55) to (57): -

$$u_{xx} = \frac{1}{c} u_t, \quad u = u(x,t), \qquad 0 < x < 1, \qquad t > 0 \tag{55}$$

$u(0,t) = u(1,t) = 0$ (boundary conditions) (56)

$u(x,0) = f(x)$ (initial condition) (57)

In order to solve the problem, x and t are discretized, as given in equations (58) and (59) below: -

$x_i = ih, \qquad i = 0,1,2,.....$ (58)

$t_j = jkj = 0,1,2,.....$ (59)

The partial differential equation (34) is approximated thus, rewritten as in equation (60): -

$$\frac{1}{2}\left(\frac{u_{i+1,j+1}-2u_{i,j+1}+u_{i-1,j+1}}{h^2}+\frac{u_{i+1,j}-2u_{i,j}+u_{i-1,j}}{h^2}=\frac{u_{i,j+i}-u_{i,j}}{ck}\right) \quad (60)$$

If the parameter r is defined, therefore r is given by an expression in equation (61) below: -

$$r=\frac{ck}{h^2}=\frac{c\Delta t}{(\Delta x)^2} \quad (61)$$

Rearranging equation (40) with all *j*+1 term on one side and j terms on the other side, we have, an expression in Equation (62):-

$$-ru_{i-1,j+1}+2(1+r)u_{i,j+1}-ru_{i+1,j+1}=ru_{i-1,j}+2(1-r)u_{i.j}+ru_{i+1,j} \quad (62)$$

The equation (62) forms the Crank-Nicholson algorithm for the partial differential equation. In order to start the process, let *j* = 0, and write the Crank-Nicholson equation for each *i* = 1,2, ..., N to obtain N simultaneous equations in N unknowns, where N is the number of interior mesh points on the row (the boundary points, with known values are excluded). The system of equations is a tridiagonal system, since each equation has three consecutive non-zeros centered around the diagonal. Also, observing the figure below, the points involve in the Crank-Nicholson scheme are shown. Starting at the bottom row (*j* = 0) and moving up, the right-hand side values of equation (62) are known and the left-hand side values are unknown. Next, with *j*=1, a new set of equation is solved. Figure 2 shows the sketch of the Crank-Nicholson stencil.

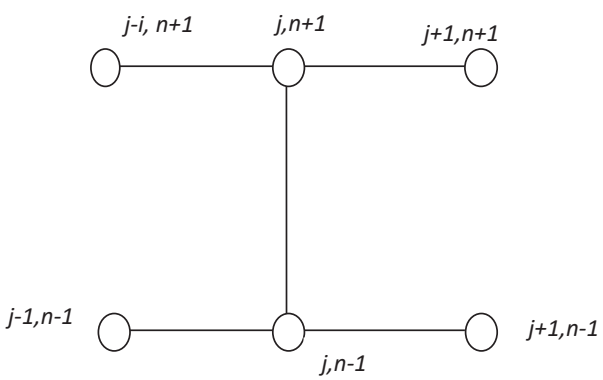


Figure 2: The Crank-Nicholson Stencil

### 4.2 Application of Crank-Nicholson Finite Difference Method to the Developed Model.

Applying the Crank-Nicholson finite difference method to the set of partial differential equations, the equations 47 and 48 could be solved alongside Initial and Boundary conditions and equilibrium relationships in equations (49 - 51). An algorithm to solve these equations was developed and implemented using a computer algorithm with MATLAB (v 7.9.0, R2009b.) (2014).

Table 1: Model Parameters used for simulation. (Pruskathorn et al., 2009)

| Symbol | Parameter | Unit | Value | |
|---|---|---|---|---|
| $\varepsilon_b$ | Bed porosity | - | 0.36 | |
| T | Temperature | K | 473 | |
| U | Velocity | cm/s | 0.00839 | |
| $\rho_p$ | particle density | g/cm$^3$ | 1.482 | |
| $D_E$ | Axial dispersion coefficient | cm$^2$/s | 1.658E-3 | |
| L | Bed height | cm | 50 | |
| $C_i$ | Inlet concentration | mol/cm$^3$ | 1.0 | |
| $K_i$ | External mass transfer coefficient | s$^{-1}$ | 0.030 | |
| | Langmuir parameter | $\frac{mmol}{g}$ | $t_{1_1}$ | 15.547 |
| | | $\frac{mmol}{gk}$ | $t_{2_1}$ | -0.0446 |
| | | $atm^{-1}$ | $t_{3_1}$ | 0.00172 |
| | | | $t_{4_1}$ | 1339.168 |

## 5.0 RESULTS AND DISCUSSION

The outlet concentration, and concentration at different bed positions and different times were determined and adsorption curves were generated. The results are presented in Tables 2 to 5, and plots shown in Figures 1 to 5.

Table 2: Fluid phase concentration of water at different bed position

| T | Exp | Z=0 | Z=0.1 | Z=0.5 | Z=1 |
|---|---|---|---|---|---|
| 0 | 0 | 1 | 0 | 0 | 0 |
| 0.1 | 0.02 | 1 | 0.014459 | 0.006925 | 0.006923 |
| 0.2 | 0.05 | 1 | 0.074718 | 0.041561 | 0.041548 |
| 0.3 | 0.15 | 1 | 0.177532 | 0.123622 | 0.123571 |
| 0.4 | 0.3 | 1 | 0.2926 | 0.227156 | 0.227036 |
| 0.5 | 0.48 | 1 | 0.410975 | 0.336748 | 0.336523 |
| 0.6 | 0.64 | 1 | 0.530195 | 0.448232 | 0.447864 |
| 0.7 | 0.78 | 1 | 0.649315 | 0.560165 | 0.559616 |
| 0.8 | 0.9 | 1 | 0.767887 | 0.671906 | 0.671136 |
| 0.9 | 1 | 1 | 0.885669 | 0.78312 | 0.782093 |
| 1 | 1 | 1 | 1 | 0.893617 | 0.892293 |

Table 3: Solid phase concentration of water at different bed position

| T | Z=0 | Z=0.1 | Z=0.5 | Z=0.7 | Z=1 |
|---|---|---|---|---|---|
| 0 | 1 | 1 | 1 | 1 | 1 |
| 0.1 | 0 | 0.996074 | 0.996074 | 0.996074 | 0.996074 |
| 0.2 | 0 | 0.966111 | 0.976412 | 0.976412 | 0.976414 |
| 0.3 | 0 | 0.911753 | 0.929731 | 0.929731 | 0.929738 |
| 0.4 | 0 | 0.850004 | 0.870558 | 0.870558 | 0.870568 |
| 0.5 | 0 | 0.785885 | 0.807548 | 0.807548 | 0.807561 |
| 0.6 | 0 | 0.72078 | 0.743038 | 0.743038 | 0.743053 |
| 0.7 | 0 | 0.65522 | 0.67784 | 0.67784 | 0.67758 |
| 0.8 | 0 | 0.58946 | 0.612316 | 0.612316 | 0.612336 |
| 0.9 | 0 | 0.52364 | 0.546656 | 0.546656 | 0.546678 |
| 1 | 0 | 0.457844 | 0.480969 | 0.480969 | 0.480994 |

Table 4: Fluid phase concentration of water at different time

| Z | t=0 | t=0.1 | t=0.5 | t=1 |
|---|---|---|---|---|
| 0 | 1 | 1 | 1 | 1 |
| 0.1 | 0 | 0.014459 | 0.410975 | 0.894096 |
| 0.2 | 0 | 0.006927 | 0.336915 | 0.893618 |
| 0.3 | 0 | 0.006925 | 0.336748 | 0.893617 |
| 0.4 | 0 | 0.006925 | 0.336748 | 0.893617 |
| 0.5 | 0 | 0.006925 | 0.336748 | 0.893617 |
| 0.6 | 0 | 0.006925 | 0.336748 | 0.893617 |
| 0.7 | 0 | 0.006925 | 0.336748 | 0.893617 |
| 0.8 | 0 | 0.006925 | 0.336748 | 0.893617 |
| 0.9 | 0 | 0.006925 | 0.336747 | 0.893616 |
| 1 | 0 | 0.006923 | 0.336523 | 0.892293 |

Table 5: Solid phase concentration of water at different time

| Z | t=0 | t=0.1 | t=0.5 | t=1 |
|---|---|---|---|---|
| 0 | 1 | 0 | 0 | 0 |
| 0.1 | 1 | 0.996074 | 0.785885 | 0.457844 |
| 0.2 | 1 | 0.996074 | 0.807528 | 0.480943 |
| 0.3 | 1 | 0.996074 | 0.807548 | 0.480969 |
| 0.4 | 1 | 0.996074 | 0.807548 | 0.480969 |
| 0.5 | 1 | 0.996074 | 0.807548 | 0.480969 |
| 0.6 | 1 | 0.996074 | 0.807548 | 0.480969 |
| 0.7 | 1 | 0.996074 | 0.807548 | 0.480969 |
| 0.8 | 1 | 0.996074 | 0.807548 | 0.480969 |
| 0.9 | 1 | 0.996074 | 0.807548 | 0.480969 |
| 1 | 1 | 0.996074 | 0.807561 | 0.480994 |

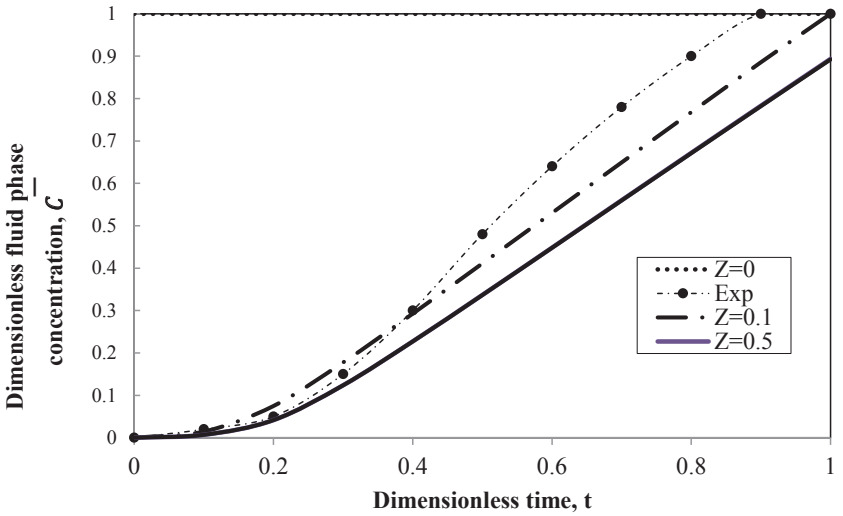


Figure 1. Plot of dimensionless fluid phase concentration of water against dimensionless time for different bed positions

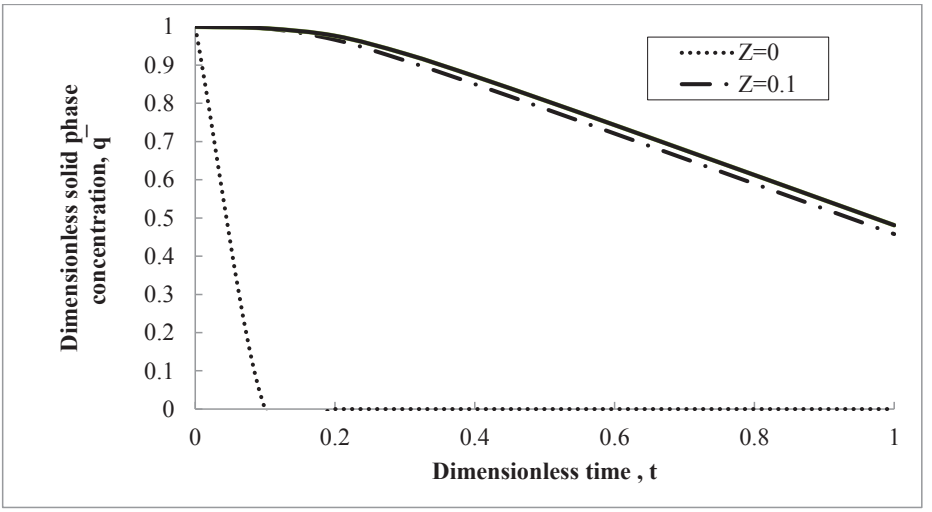


Figure 2. Plot dimensionless solid phase concentration of water against dimensionless time for different bed positions

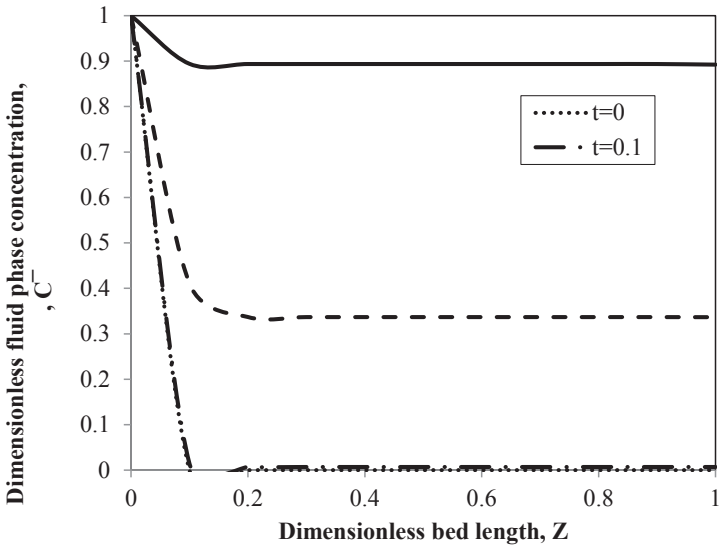


Figure 3. Plot of dimensionless fluid phase concentration of water against dimensionless bed length at different time

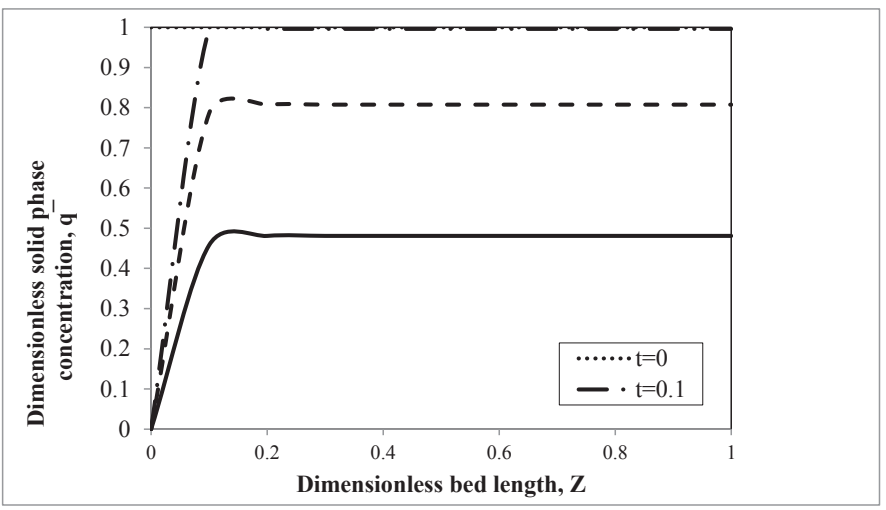


Figure 4.Plot of dimensionless solid phase concentration of water against dimensionless bed length at different time

The adsorbent has a stronger affinity for water in the ethanol-water system as its average pore size allows the entrance of water molecule. The ethanol molecular size is larger than the pore size of the sieve. There is alcohol concentration increase as water uptake was found to be higher in the first hour. This can be seen in Figure 1. The curve obtained from the simulated data for z =0.1 follows the pattern of the

experiment as they have the same dimensionless fluid phase concentration of 0.29 at dimensionless time of 0.39 (2384 sec or 39 min 44 sec). Also the Least Sum of Square Residuals (LSSR) of z = 0.1 is 0.06588 while that of z = 1.0 is 0.223799 which further shows that z = 0.1 correlates the experimental data.

There is also steady increase of water concentration in the solid along the bed length. Comparing the behavior of the simulated data with the experimental data, in Figure 1, it could be seen that a bed length of z = 0.1, a breakthrough time of dimensionless time of t = 0.1 (600 seconds i.e.10 minutes) obtained from the simulated result, showed a breakthrough time of 680 seconds (11 minutes, 20 seconds) similar to what was reported in the experimental result. The similarities in these results show that the developed model adequately represent the experimental data.

In Figure 2, it could be seen that there is steady increase of water concentration in the solid phase until saturation point and there is no adsorption of water any longer. This saturation occurred at the simulated breakthrough time of 600 seconds, the solid phase concentration falls gradually. As the bed becomes saturated at that point, regeneration becomes necessary.

Figure 3, the plot of the dimensionless fluid phase concentration against dimensionless bed position, shows that the concentration of water in the fluid phase decreases along the bed and then becomes constant this confirms that the bed has become saturated with water. It is also observed that the constant concentration obtained after a linear decline was lower for dimensionless t = 0.1 than for t = 0.5 and t = 1.0.

Figure 4 shows a behavior that validates the occurrence in Figure 3. The concentration in the solid phase increased to a maximum and becomes constant (when the bed is saturated).

## 7.0 CONCLUSION

The results of the adsorption show that Crank Nicholson finite difference technique developed in MATLAB was able to handle the solution of the model. The result is in agreement with reported experimental data in literature. The breakthrough time of 600sec was obtained for this work as compared to 680sec reported in literature. Also, there was a closeness in curve pattern in the breakthrough curve for dimensionless bed position of z = 0.1 (with LSSR of 0.06588) and the experimental data.

The disparity in the result could be attributed to some of the assumptions made in the model development. These include: single component adsorption, isothermal condition, adjusted Langmuir isotherm, constant velocity and negligible radial gradient. The numerical method used for computation was quite efficient in providing solutions to models of this nature. Furthermore, the study gives us a better understanding of the behavior of the adsorption column for a binary system of ethanol and water, using a zeolite 3A adsorbent. The purity of 99.2705% v/v anhydrous ethanol was obtained.

**Nomenclature**

| | |
|---|---|
| å | external surface area of the particles per unit volume of the bed, m |
| b | Langmuir parameter, atm |
| $C_f$ | fluid phase concentration, mol/cm' |
| $D_E$ | axial dispersion coefficient, m'/sec |
| $J_o$ | solute flux to the surface of the pellet from the fluid phase, mol/$m^2$.s |
| $k_i$ | external film mass transfer coefficient, cm/s |
| Pe | Peclet number |
| qm | Langmuir parameter, mol/g |
| $q_i$ | amount of component i adsorbed on the solid phase |
| $q_i$" | amount of component i adsorbed in equilibrium with fluid phase, mol/g |
| R | gas constant, cm3 atm/gmol.K |
| t | time, sec |
| $\bar{t}$ | dimensionless time |
| $t_1$ | Langmuir parameter, mol/g. |
| $t_2$ | Langmuir parameter, mol/g.K |
| $t_3$ | Langmuir parameter, atm-1 |
| $t_4$ | Langmuir parameter, K |
| T | Temperature, K |
| U | Interstitial velocity, cm/s |
| z | dimensional bed position, cm |
| $\bar{z}$ | dimensionless bed position |
| $\varepsilon_b$ | bed porosity |
| $\rho_b$ | particle density, g/$cm^3$ |
| * | equilibrium value |

## REFERENCES

Al-Malah, K. I. M., (2014). Matlab. *Numerical methods with chemical engineering applications*. New York:McGraw-Hill Education.

Chopade, V. J., Khadetoid, Y. P. & Mohod, A. G. (2015). Dehydration of Ethanol-Water Mixture Using 3A Zeolite Adsorbent, *International Journal of Engineering Technology and Emerging and Advanced Engineering*, 5(11):152 – 155.

Baylak, T., Kumar, P., Niu, C. H. & Dalai, A., (2012). Ethanol Dehydration in a Fixed Bed Using Canola Meal. *Energy Fuels 26*(8): 5226 – 5231.

Delgado, J. A., Agueda, V. I., Uguma, M. A., Sotelo, J. I., Gacia-Sanz, A & Garcia, A. (2015). Separation of Ethanol-Water Liquid Mixtures by Adsorption on BPL Activated Carbon with Air Generation. *Separation and Purification Technology*, 149: 370-380.

Elzbieta, G., Nastaj, J., Tabero, P. & Aleksandrzak, T., (2015). Experimental studies on 3A and 4A zeolites molecular sieves regeneration in TSA process. Aliphatic alcohols dewatering—water desorption. *Chemical Engineering Journal*, 259: 232-242.

Grande, C. A. & Blom, R. (2012). Dual pressure swing adsorption units for gas separation and purification. *Industrial & Engineering Chemistry Research*, 51: 8695–8699.

J-Jeong, J. S., Jeon, H, Ko, K. M., Chung, B. & Choi, G. W. (2012). Production of anhydrous ethanol using various pressure swing processes in pilot plant. *Renewable Energy* 42: 41-45.

Jochen J. & Helmut, S. (2012). Adsorption properties of porous materials for solar thermal energy storage and heat pump applications. *Energy Procedia* 30: 289 – 293.

Mazumder, S.. (2015). *Numerical Methods for Partial Differential Equations (1st ed.). Finite Difference and finite Volume Methods*. Academic press.

Okewale, A. O., Igbokwe, P. K. & Ogbuagu, J. O. (2013). Kinetics and isotherm studies of the adsorptive dehydration of ethanol-water with biomas based materials. *International Journal of Engineering and Innovative Technology*, 2(9): 36-42.

Pruksathorn, P. & Vitidsant, T. (2009). Production of pure ethanol from azeotropic solution by pressure swing adsorption. *American Journal of Engineering and Applied Sciences* 2, (1): 1-7.

Saengduan, P. & Apichat, B. (2011). Process optimization for motor fuel Grade ethanol production using hybrid vapor permeation and pressure swing adsorption technique. *European Journal of Scientific Research* 64: 644-657.

Seader, J. D., Henley, E. J. & Roper, D. K. (2011) *Separation Process Principles:chemical and biochemical operations,* (3rd ed.) USA John Wiley & Sons Inc.